Chapter 4

Non-premixed turbulent flames using RANS models and flamelet modelling approaches

4.1 Introduction

In technical equipment such as engines, boilers, and furnaces, combustion nearly always takes place within a turbulent rather than a laminar flow field. This fact respond to two main reasons. First, turbulence increases the mixing and transport processes and thereby enhances combustion. Second, combustion releases heat and as a result generates flow instability by buoyancy and gas expansion, which then enhances the transition to turbulence [1]. As a consequence of the enhancement of the mixing process, combustion chambers are, for example, much smaller than those possible with laminar flows [2].

Much remains to be investigated about turbulent fluid flow by itself, and the addition of chemical kinetics with energy release only further complicates an already difficult problem [2]. Direct Numerical Simulation (DNS) using full 3D integration and time dependent governing equations (equations presented in the introduction chapter) is generally restricted to simple geometries and low Reynolds numbers due to the large, if not prohibitive, computational resources required in terms of CPU time and memory [3]. Turbulence modelling based on volume filtering, the so-called Large Eddy Simulation (LES) [4], is a relatively young technique and still requires large computational resources (less than DNS, but still large). RANS models (Reynolds-Averaged Navier-Stokes Simulations) based on a time-averaging of the dependent variables and the governing equations, have received greater attention in the past

decades due to their wide range of application and reasonable computational cost. This technique solves both the large and small eddies, taking a time-averaged of the variables. The new unknowns that appear as a consequence of the time-averaging of the equations require what is known as *turbulence models*. Different possibilities to evaluate these terms can be applied [3, 5]: i) Differential Reynolds Stress models (DRSM), where a differential equation for each unknown is derived; ii) Algebraic Reynolds Stress models (ARSM), which convert the differential equations to algebraic equations; iii) Eddy Viscosity models (EVM), where a turbulent viscosity is defined and applied in addition to the molecular one [6].

Eddy viscosity models, and specially the two-equation version, have been widely used for both fundamental and applied researches of turbulent flows. Turbulent combustion flows have been also successfully and widely modelled with EVM. However, and arising from the mathematical formulation implicit with EVM, an important issue to be understood in turbulent combustion, in addition to the turbulent structures of the flow, is the turbulence/chemistry interaction. This is one of the key difficulties in the mathematical modelization and different possibilities are proposed in the literature.

In the present thesis, and taking advantage of the knowledge and experience achieved in the previous chapter, the application of the laminar flamelet concept for turbulent combustion with a presumed probability density function for the mixture fraction variable is explored using an eddy-viscosity two-equation turbulent model. In addition, simpler models such as Eddy Dissipation Models (EDM) [7] which assumes fast chemistry usually restricted to simple chemistry, are also applied and compared with flamelet modelizations. In order to apply these methodologies to turbulent combustion, there are different flame configurations that can be selected. The flames explored in the framework of the *International Workshop on Measurement and Computation of Turbulent Non-premixed Flames* (TNF) [8] are specially suitable to analyse phenomenological characteristics and basic aspects of mathematical models. Since the main feature to be investigated in the present chapter is the application of the flamelet concept to turbulent combustion, a simple configuration of the structure of flow is selected to reduce uncertainties due to the turbulent modelling of the flow. The selected case is the well-known piloted methane/air turbulent jet flame so-called Flame D [8, 9] which is a non-confined jet. Extensive experimental data available in the literature for the Flame D test case has been considered for validation purposes.

4.2 Turbulence characterisation

4.2.1 General trends

Turbulent flows are transitory, highly diffusive, three-dimensional, irregular, seemingly random, chaotic and present many scales of motion [6]. Thus, this is a complex phenomenon and its complete comprehension is still to come. The goal of this section is to give a brief description of the physical characterisation of the turbulence phenomenon, its origin, the main physical features, and the consequences from the engineering point of view. Nevertheless, many text books can be found for further reading and understanding of this complex phenomenon. Among others, and as an example, see [3, 5, 10].

The irregular nature of turbulence stands in contrast to laminar motion, so called historically, because the fluid was imagined to flow in smooth laminae, or layers. Careful analyses of solution to the Navier-Stokes equations show that turbulence develops as an instability of a laminar flow. In principle, the time-dependent, three-dimensional Navier-Stokes equations contains all of the physics of a given turbulent flow. This follows from the fact that turbulence is a continuum phenomenon. However, the inherent non-linearity of the Navier-Stokes equations precludes a complete analytical description of the actual transition process from laminar to turbulent regime. The instabilities result from interactions between the Navier-Stokes equations nonlinear inertial terms and viscous terms (inertial forces and viscous forces) [5]. This interaction is very complex because it is rotational, fully three-dimensional and time dependent, leading to a wide range of excited time and length scales. A continuous spectrum of scales ranging from the largest to the smallest can be observed.

Turbulent flows always occur for high Reynolds numbers. For high Reynolds numbers, the energy-cascade model of Kolmogorov establishes a transport of the kinetic energy from the main flow to the bigger vortexes or eddies. These eddies are characterised by length scales with the same order of magnitude of the main flow, with a high level of anisotropy and with low fluctuation frequencies. A turbulent eddy can be thought of as a local swirling motion whose characteristic dimension is the local turbulence scale. Eddies overlap in space, large ones carrying smaller. Then, as the turbulence decays, its kinetic energy transfers from larger eddies to smaller ones. In this process, the kinetic energy goes from larger to smaller vortexes until it is dissipated and converted to internal energy by means of the viscous forces (molecular viscosity). Thus, turbulence flows are always dissipative. These smaller scales (dissipative or Kolmogorov scales) are characterised by high fluctuation frequencies and isotropic structures. In some situations, an inversion of the energy-cascade process from smaller to the larger scales can also occur (backscatter) [11].

The interaction between the vortexes leads to a stretching process (known as vortex stretching) that reduces their diameter increasing their angular velocity. Stretch-

ing a vortex along its axis will make it rotate faster and decrease its diameter in order to maintain its kinetic momentum constant. Vigorous stretching of vortex lines is required to maintain the ever-present fluctuating vorticity in a turbulent flow.

The strongly rotational nature of turbulence goes hand-in-hand with its three-dimensionality. This inherent three-dimensionality means that there are no satisfactory two-dimensional approximations. The time-dependent nature of turbulence also contributes to its intractability. Turbulence is characterised by random fluctuations making difficult a deterministic approach to the problem. Rather, statistical methods must be used.

Perhaps the most important feature of turbulence from an engineering point of view is its enhanced diffusivity. Turbulent diffusion greatly enhances the transfer of mass, momentum and energy. The effectiveness of turbulence for transporting and mixing fluids is of prime importance in many applications. When different fluid streams are brought together to mix, it is generally desirable for this mixing to take place as rapidly as possible. This is certainly the case for pollutant streams released into the atmosphere and for the mixing of different reactants in combustion devices and chemical reactors [3].

4.2.2 Statistical description of turbulent flows. The random nature of turbulence

The governing equations described in section 1.3.1 are equally applied to laminar and turbulent flows, but in turbulent regimes, the primitive variables that describe the flow such as velocity, temperature and mass fractions behave like *random variables*. This means that a generic variable ϕ does not have a unique value, the same every time the experiment is repeated under the same set of conditions [3]. Every time the experiment is repeated, ϕ takes a different value. It does not mean that turbulence is a random phenomenon. Turbulence is governed by deterministic equations but the solutions are random variables. The consistency of this statement lies in the combination of two factors: i) in turbulent flows there are unavoidable perturbations in initial conditions, boundary conditions and material properties; ii) turbulent flows exhibit a high sensitivity to such perturbations. The perturbations are also present in laminar flows but in turbulent flows, the evolution of the flow is extremely sensitive to small changes of the specified conditions [3].

Therefore, since turbulence is described by random variables, their values are inherently unpredictable. However, mathematical tools that characterise random variables must be introduced. The *probability density function* (pdf) completely characterise a random variable and it serves to represent a probability distribution in terms of integrals. Two important quantities to highlight are the mean (probability-weighted average) and the variance (mean-square fluctuation) of a random variable.

The square-root of the variance is the standard deviation. Given a random variable ϕ and its probability density function $P(\phi)$, the mean $\overline{\phi}$ and the variance $\overline{\phi'^2}$ are evaluated as follows:

$$\overline{\phi} = \int_{-\infty}^{+\infty} \phi P(\phi) d\phi \tag{4.1}$$

$$\overline{\phi'^2} = \int_{-\infty}^{+\infty} (\phi - \overline{\phi})^2 P(\phi) d\phi \tag{4.2}$$

In the following sections, these concepts and these two quantities will be of special interest in order to construct capable and useful turbulent models.

4.2.3 Turbulent combustion

Turbulent combustion results from the interaction of chemistry and turbulence. When a flame interacts with a turbulent flow, turbulence is modified by combustion because of the strong flow accelerations through the flame front induced by heat release, and because of the large changes in kinematic viscosity associated with temperature changes. This mechanism may generate turbulence or damp it (re-laminarization due to combustion). On the other hand, turbulence alters the flame structure, may enhance chemical reactions increasing the reactions rates but also, in extreme cases, completely inhibit it, leading to flame quenching [12].

Combustion, even without turbulence, is an intrinsically complex process involving a large range of chemical time and length scales. Combustion processes usually involve a large chemistry mechanism with a very large number of species and reactions (i.e. for methane, GRI-Mech of 53 species and 325 reactions) that take place in a wide range of time scales. In many chemically reacting flows, chemical processes occur with time scales differing by many orders of magnitude (e.g. 10^{-10} s to 1 s in combustion processes), whereas the time scales of flow, molecular transport, and turbulence usually cover a much smaller range of time scales [2]. Since turbulence is inherently transient, all the characteristic time scales must be retained in order to capture and describe the phenomenon. Therefore, in combustion systems the faster reactions impose a very fine time resolution. In order to avoid this severe limitation, many research has been focused on the reduction of the detailed chemical mechanisms to eliminate faster reactions as well as the number of chemical species involved.

4.3 Turbulence Modelling

Direct Numerical Simulation (DNS) of turbulent reactive flows where all the spatial and temporal scales must be solved without any introduction of empirical information, is limited to few cases due to the huge computational costs involved. In addition, and

as a result of the inherent time-dependent nature of a turbulent flow, the chemistry also must be resolved properly considering all the reactions, from the slowest to the fastest.

From these limitations arises the need of using statistical techniques to model the turbulent flows. An ideal model should introduce the minimum amount of complexity while capturing the essence of the relevant physics [5]. The principal criteria that can asses different models are: i) level of description; ii) completeness; iii) cost and ease of use; iv) range of applicability, and v) accuracy [3]. Mainly, there are three different statistical techniques to face turbulence modelling:

- Large Eddy Simulations (LES): Based on the volume-averaged of the governing equations. The averaging process (filtering) is only carried out for the smaller turbulent scales, while the three-dimensional and transient structure of the larger turbulent scales are simulated in detail. As small scales are characterised by an isotropic structure (at least for high Reynolds numbers) and are more universal, they are easier to be modelled. These small turbulent eddies are modelled using a sub-grid model. LES models reduce the space and time grids needed for DNS resolutions, but still require large computational resources for routine simulations. Even though, they are a promising tool and the scientific community is devoting time and resources to these models given the ever-increasing computational resources. See further information in [4].

- Reynolds Averaged Navier-Stokes Simulations (RANS): This technique solves the governing equations by modelling both the large and the small eddies, taking a time-averaged of variables. The information supplied by these models is the time-average of the variables and the fluctuating parts are not represented directly by the numerical simulation, and are included only by means of a turbulence model. These models have been extensively used for scientific and engineering calculations during the last decades. They are specially designed for high Reynolds number and distinguishable separation of the time-scales related to the fluctuating behaviour of the variables and the time-scales related to the main flow unsteady behaviour. The main advantage is the relatively low computational cost involved compared to DNS or LES calculations. The bottle-neck of these modelizations is the difficulty to obtain highly accurate in addition to universally applicable models.

- The PDF transport equation model: This stochastic method consist of considering the probability distribution of the relevant stochastic quantities directly by means of probability density functions (pdf). In turbulent flows, the pdf P is a function of both, the position x and the time t. Then, $P(U; x, t)$ denotes de probability of finding a value u within the range $U \leq u \leq U + dU$ at the location x and time t [13]. One of the most common PDF models used is a

joint PDF transport equation for the velocity and the scalars [14]. For reactive flows, the reactive scalars are considered, say temperature and species mass fractions. This models represent a very general statistical description of turbulent reactive flows, applicable to premixed, non-premixed, and partially premixed combustion [1]. The chemical reactions rates are exact without any modelling at all in the PDF transport equation. The closure problem is shifted to the mixing of scalar gradients. A complete discussion of these models can be found in [3, 14]. From a numerical point of view, the most apparent property of the PDF transport equation is its high dimensionality. Finite-volume techniques are not very attractive for this type of problem as the memory requirements increase roughly exponentially with dimensionality. Therefore, numerical implementations of PDF methods for turbulent reactive flows employ Monte-Carlo simulation techniques which employ a large number of particles (N) [1, 14]. The particles should be considered as different realizations of the turbulent reactive flow problem and should not be confused with real fluid elements. The state of a particle is described by its position and velocity, and the values of the reactive scalars.

4.4 RANS modelling

4.4.1 Time-averaging

In order to introduce the concept of time-averaging, each instantaneous variable of the system (e.g. ϕ) is decomposed in two parts: a mean part usually denoted with an over-bar $\overline{\phi}$; and a fluctuating part ϕ':

$$\phi = \overline{\phi} + \phi' \tag{4.3}$$

RANS models assume a separation of the fluctuating time scales of the variables t_1 and the main time scale characteristic of the "slow" variation of the mean flow t_2. This means that time scales t_1 and t_2 exist and differ by several orders of magnitude, $t_1 << t_2$, otherwise the mean and fluctuation components would be correlated. The decomposition in an averaged and a fluctuation part would not be appropriate for such flows where there is no distinct boundary between the unsteadiness and turbulent fluctuations [5]. For a time-dependent mean variables, assuming a "short-time" averaging, and for a period Δt which $t_1 < \Delta t < t_2$, the time-averaged variable is defined as:

$$\overline{\phi}(\vec{r}, t) = \overline{\phi} = \frac{1}{\Delta t} \int_t^{t+\Delta t} \phi(\vec{r}, t')dt' \tag{4.4}$$

The mean of the fluctuating part can be set to zero:

$$\overline{\phi'} = 0 \tag{4.5}$$

Large density variations are typical for combustion processes. As a consequence, the classical approach to model turbulent flows with time-averaging techniques [5, 15–17] is formally extended to include non-constant density effects by introducing density-weighted averages (also called Favre-averages). This kind of average allows a much more compact formulation with fewer unknown correlations in the process of deduction of the averaged Navier-Stokes equations. Given an arbitrary property ϕ, its Favre-averaged, denoted with $\widetilde{\phi}$, is given by:

$$\widetilde{\phi} = \frac{\overline{\rho\phi}}{\overline{\rho}} \tag{4.6}$$

Then, the separation of the instantaneous variable again can be split into its mean value and the fluctuations

$$\phi = \widetilde{\phi} + \phi'' \tag{4.7}$$

Here, the result for the average of the Favre-fluctuation is:

$$\overline{\rho\phi''} = 0 \tag{4.8}$$

This result is obtained taking into account Eq. 4.6 and developing the $\overline{\rho\phi}$ as follows:

$$\overline{\rho\phi} = \overline{\rho\left(\widetilde{\phi} + \phi''\right)} = \overline{\rho}\overline{\widetilde{\phi}} + \overline{\rho\phi''} = \overline{\rho}\widetilde{\phi} + \overline{\rho\phi''} \tag{4.9}$$

The density-weighted averages or Favre-averages require the density as a factor to weight the variable:

$$\overline{\rho}(\vec{r},t)\widetilde{\phi}(\vec{r},t) = \overline{\rho}\widetilde{\phi} = \frac{1}{\Delta t}\int_t^{t+\Delta t} \rho(\vec{r},t')\phi(\vec{r},t')dt' \tag{4.10}$$

where:

$$\overline{\rho}(\vec{r},t) = \frac{1}{\Delta t}\int_t^{t+\Delta t} \rho(\vec{r},t')dt' \tag{4.11}$$

4.4.2 Favre-averaged transport governing equations

Applying the definition of Eq. 4.6 into the governing equations with instantaneous variables defined in the introduction chapter (Eqns. 1.1, 1.2, 1.3 and 1.6) and averaging the resulting equations, the following Favre-averaged equations can be written:

$$\frac{\partial\overline{\rho}}{\partial t} + \nabla\cdot\left(\overline{\rho}\widetilde{\vec{v}}\right) = 0 \tag{4.12}$$

$$\frac{\partial\left(\overline{\rho}\widetilde{Y_i}\right)}{\partial t} + \nabla\cdot\left(\overline{\rho}\widetilde{\vec{v}}\widetilde{Y_i}\right) = -\nabla\cdot\overline{\vec{j}_i} - \nabla\cdot\left(\overline{\rho}\widetilde{\vec{v}''Y_i''}\right) + \overline{\dot{w}_i} \tag{4.13}$$

$$\frac{\partial\left(\overline{\rho}\widetilde{\vec{v}}\right)}{\partial t}+\nabla\cdot\left(\overline{\rho}\widetilde{\vec{v}}\widetilde{\vec{v}}\right)=\nabla\cdot\overline{\vec{\tau}}-\nabla\cdot\left(\overline{\rho}\widetilde{v''\vec{v}''}\right)-\nabla\overline{p}+\overline{\rho}\vec{g} \tag{4.14}$$

$$\frac{\partial\left(\overline{\rho}\widetilde{h}\right)}{\partial t}+\nabla\cdot\left(\overline{\rho}\widetilde{\vec{v}}\widetilde{h}\right)=-\nabla\cdot\overline{\vec{q}}-\overline{\nabla\cdot\vec{q}^{\,R}}-\nabla\cdot\left(\overline{\rho}\widetilde{v''h''}\right) \tag{4.15}$$

These equations show that as a result of the averaging process and the non-linearity of the convective terms, Favre-averaged products of fluctuating variables appear as new unknowns, while molecular terms, the radiation heat term and the reaction rate appear time-averaged. A treatment for these terms is required.

In the following subsections different alternatives to model these unknowns are explored giving idea of the assumptions considered and the inherent difficulties that appear in this modelization process.

4.4.3 Reynolds stresses and scalar turbulent fluxes

These terms correspond to the convective transport of momentum, mass and energy due to the fluctuating component [11]: Reynolds stresses $\overline{\rho}\widetilde{\vec{v}''\vec{v}''}$ and scalar turbulent fluxes $\overline{\rho}\widetilde{\vec{v}''Y_i''}$ and $\overline{\rho}\widetilde{\vec{v}''h''}$.

The averaging process obviously leads to a loss of some of the information contained within the instantaneous equations. This lack of information is overcome by means of approximations of those unknown terms as a function of the averaged variables. This is the so-called *closure problem* of turbulence RANS models. There are different alternatives to face up to the problem, depending on the degree of modelization employed and the hypothesis assumed. A further read of different approaches can be found, among others, in [3] and [5].

In this thesis, the so-called Eddy Viscosity Models (EVM) are employed because they combine generality, reasonable accuracy, simplicity and acceptable computation effort. They are the most extended models in engineering calculations and they are considered the simplest complete models of turbulence since no prior knowledge of the turbulence structure is required. These models are based on an addition of an isotropic turbulent (or eddy) viscosity μ_t to the molecular viscosity inherent to the Newtonian fluids. Basically, the idea is to enhance the transport of a variable by a diffusion coefficient defined by analogy to the Stoke's law of viscosity. Then, the turbulent stresses are defined by:

$$\overline{\rho}\widetilde{\vec{v}''\vec{v}''}=-2\mu_t\widetilde{\vec{\gamma}}-\frac{2}{3}\left(\mu_t\nabla\cdot\widetilde{\vec{v}}\right)\vec{\delta}+\frac{2}{3}\overline{\rho}\widetilde{k}\vec{\delta} \tag{4.16}$$

where $\widetilde{\vec{\gamma}}$ is the Favre-averaged rate of strain tensor (see Eq. 1.10); $\widetilde{k}$ is the Favre-averaged turbulent kinetic energy and $\vec{\delta}$ is the Kronecker Delta. The second term of

the r.h.s ($\frac{2}{3}\overline{\rho}\widetilde{k}\vec{\delta}$) is needed to obtain the proper trace of the Reynolds stress tensor.

The kinetic energy (per unit mass) of the turbulent fluctuations is the basis of the velocity scale and is a key variable in the definition of a turbulent flow. It can be defined as a half of the sum of the trace of the Reynolds stress tensor ($\frac{1}{2}\overline{\vec{v''}\cdot\vec{v''}}$). However, in Eq. 4.16 and given the fluctuations of density in combustion processes, it is useful to define the Favre-averaged turbulent kinetic energy as:

$$\widetilde{k} = \frac{1}{2}\widetilde{\vec{v''}\cdot\vec{v''}} \tag{4.17}$$

For the scalar turbulent fluxes it is commonly assumed the *simple gradient diffusion hypothesis*, not only for non-reacting scalars but also for reactive scalars. The turbulent scalar flux is assumed to be aligned with the mean scalar gradient. The turbulent diffusion coefficient is usually considered proportional to the turbulent viscosity by means of the definition of a turbulent Prandtl number for each scalar (i.e σ_h, σ_{Y_i}), which are constants of the turbulent models. Then, the turbulent scalar fluxes are defined as:

$$\overline{\rho}\widetilde{\vec{v''}h''} = -\frac{\mu_t}{\sigma_h}\nabla\widetilde{h} \tag{4.18}$$

$$\overline{\rho}\widetilde{\vec{v''}Y_i''} = -\frac{\mu_t}{\sigma_{Y_i}}\nabla\widetilde{Y_i} \tag{4.19}$$

Therefore, the key problem is the evaluation of the turbulent viscosity. The most extended possibility is based on the resolution of two transport equations properly modelled: the equation for the turbulent kinetic energy, and another equation accounting for the dissipation of the turbulent kinetic energy. Different variables can be used for the dissipation of the turbulent kinetic energy. Among others, Favre-averaged dissipation rate $\widetilde{\epsilon}$ or Favre-averaged specific dissipation $\widetilde{\omega}$ are the most commonly used. Specially the $\widetilde{\epsilon}$ variable, which leads to the the so-called $\widetilde{k}-\widetilde{\epsilon}$ models in the context of eddy-viscosity two-equation models, are used. Hereinafter, the attention is focused to these models.

The turbulent viscosity is obtained from dimensional analysis or from analogy to the molecular viscosity as $\mu_t \propto \overline{\rho} v_t l$. The characteristic velocity v_t is defined by $\widetilde{k}^{1/2}$, and the length scale l is obtained from $\widetilde{k}^{3/2}/\widetilde{\epsilon}$ (or $\widetilde{k}^{1/2}/\widetilde{\omega}$ for $\widetilde{k}-\widetilde{\omega}$ models). Then,

$$\mu_t = C_\mu f_\mu \overline{\rho}\frac{\widetilde{k}^2}{\widetilde{\epsilon}} \tag{4.20}$$

Here, C_μ is an empirical constant and f_μ is an empirical damping function introduced to account for those zones with low turbulent Reynolds numbers.

The transport equations for the turbulent Favre-averaged variables $\widetilde{k}$ and $\widetilde{\epsilon}$ can be written as:

$$\frac{\partial\left(\overline{\rho}\widetilde{k}\right)}{\partial t}+\nabla\cdot\left(\overline{\rho}\widetilde{\vec{v}}\widetilde{k}\right)=\nabla\cdot\left[\left(\mu+\frac{\mu_t}{\sigma_k}\right)\nabla\widetilde{k}\right]+P_k-\overline{\rho}\widetilde{\epsilon} \tag{4.21}$$

$$\frac{\partial\left(\overline{\rho}\widetilde{\epsilon}\right)}{\partial t}+\nabla\cdot\left(\overline{\rho}\widetilde{\vec{v}}\widetilde{\epsilon}\right)=\nabla\cdot\left[\left(\mu+\frac{\mu_t}{\sigma_\epsilon}\right)\nabla\widetilde{\epsilon}\right]+c_{\epsilon1}f_1\frac{\widetilde{\epsilon}}{\widetilde{k}}P_k-c_{\epsilon2}f_2\overline{\rho}\frac{\widetilde{\epsilon}^2}{\widetilde{k}} \tag{4.22}$$

where σ_k, σ_ϵ, $c_{\epsilon1}$ and $c_{\epsilon2}$ are empirical constants of the turbulence model; f_1 and f_2 are empirical functions and P_k is the shear production of the turbulent kinetic energy evaluated as:

$$P_k=-\overline{\rho}\widetilde{\vec{v}''\vec{v}''}:\nabla\widetilde{\vec{v}} \tag{4.23}$$

A large number of proposed models can be found in the literature, i.e. [5, 16–18]. Some of these models are compiled, for instance, in [5, 15].

Most of the flames studied in this thesis correspond to axialsymmetric flow structures. These flames present for turbulent flows the so-called round-jet anomaly described in the literature [19]. Different alternatives can be considered. Most of them consist of a modification of the $c_{\epsilon2}$ constant. For instance, and as described in some posters presented in the *International Workshop on Measurement and Computation of Turbulent Non-premixed Flames* (TNF) [8], a simply modification of the standard value $c_{\epsilon2}=1.92$ for $c_{\epsilon2}=1.8$ can be considered. On the other hand, the Pope correction for this term [19] can also be used:

$$c_{\epsilon2}\frac{\widetilde{\epsilon}^2}{\widetilde{k}}\rightarrow\left[c_{\epsilon2}-c_{\epsilon3}\xi\right]\frac{\widetilde{\epsilon}^2}{\widetilde{k}} \tag{4.24}$$

where the model constant $c_{\epsilon3}=0.79$ and ξ is a non-dimensional measure of the vortex stretching. For axialsymmetric flows without swirl:

$$\xi=\frac{1}{4}\left(\frac{\widetilde{k}}{\widetilde{\epsilon}}\right)^3\left(\frac{\partial\widetilde{v_z}}{\partial r}-\frac{\partial\widetilde{v_r}}{\partial z}\right)^2\frac{\widetilde{v_r}}{r} \tag{4.25}$$

where $\widetilde{v_z}$ is the axial component of the velocity; $\widetilde{v_r}$ is the radial component of the velocity; z is the axial coordinate and r is the radial coordinate.

4.4.4 Molecular terms averaging

The averaged molecular terms such as $\overline{\vec{j}_i}$, $\overline{\vec{\tau}}$ and $\overline{\vec{q}}$ for species, momentum and energy respectively can be neglected against turbulent transport terms, assuming a sufficiently large turbulence level (large Reynolds number limit). Nevertheless, they can also be retained in order to better account near-wall zones or laminarization zones where molecular effects are important. In this thesis, mass, momentum and

energy molecular transport terms are modelled by means of expressions 1.8, 1.9 and 1.11 respectively. Taking into account these expressions, the time-averaged molecular transport terms can be modelled as [12]:

$$\overline{\vec{j}_i} = \overline{-\rho \mathcal{D}_{im} \nabla Y_i - D_i^T \nabla \ln T} \approx -\overline{\rho}\,\overline{\mathcal{D}_{im}} \nabla \widetilde{Y}_i - \overline{D_i^T} \nabla \ln \widetilde{T} \tag{4.26}$$

$$\overline{\vec{\tau}} = \overline{2\mu\vec{\gamma} - \frac{2}{3}\left(\mu \nabla \cdot \vec{v}\right)\vec{\delta}} \approx 2\overline{\mu}\widetilde{\vec{\gamma}} - \frac{2}{3}\left(\overline{\mu}\nabla \cdot \widetilde{\vec{v}}\right)\vec{\delta} \tag{4.27}$$

$$\overline{\vec{q}} = \overline{-\lambda \nabla T + \sum_{i=1}^{N} h_i \vec{j}_i} \approx -\overline{\lambda}\nabla \widetilde{T} + \sum_{i=1}^{N} \overline{h_i}\,\overline{\vec{j}_i} \tag{4.28}$$

where $\overline{\mathcal{D}_{im}}$, $\overline{D_i^T}$, $\overline{\mu}$ and $\overline{\lambda}$ are "mean" molecular diffusion coefficients. In this thesis, they are evaluated simply with the Favre-averaged temperature ($\widetilde{T}$) and the Favre-averaged species ($\widetilde{Y}_i$). The averaged enthalpy for each species $\overline{h_i}$ is evaluated considering again the Favre-averaged temperature $\widetilde{T}$. Here, the possible correlation between the fluctuating molecular viscosity, conductivity or mass diffusion coefficient has been assumed negligible.

4.4.5 Radiation term averaging

There is a lot of experimental and theoretical evidence that the Turbulence/Radiation Interaction (TRI) has a significant influence due to the temperature and species concentration fluctuations and the non-linear relationship among temperature, radiative properties and radiation intensity [20]. Despite of this, most of the works neglect such interactions. At present, the most accurate way to simulate TRI seems to be the stochastic approach even though it is very time-consuming. Some simplifications of the method can be also found in the literature. Further reading can be found in [20].

In the present thesis, the Turbulence/Radiation Interaction (TRI) is considered a second order effect and then neglected. Therefore, the time-average of the radiation heat term ($\overline{\nabla \cdot \vec{q}^{\,R}}$) is simply modelled by a substitution in the radiation model (i.e. optically thin approximation) the instantaneous temperature and species mass fractions by their Favre-averaged values.

4.4.6 Reaction rate averaging

The time-averaged reaction rate $\overline{\dot{w}_i}$ that appears as a source term in the Favre-averaged species equation (Eq. 4.13) is a key problem in turbulent combustion modelling. The instantaneous net rate of production of each species is given in the introduction chapter by Eq. 1.26. The reaction rate is highly non-linear (see Arrhenius

law) and the averaged reaction rate cannot be easily expressed as a function of the Favre-averaged mass (or molar) fractions and the Favre-averaged temperature. A simple substitution of the instantaneous mass (or molar) fractions and the instantaneous temperature by their Favre-averaged value leads to unacceptable errors. See [2] and [12] for further details. Moreover, the substitution of the instantaneous variables by their Favre-averaged in addition to their fluctuating component ($Y_i = \widetilde{Y}_i + Y_i''$ and $T = \widetilde{T} + T''$) leads to new unknown correlations very difficult to be modelled [21].

To model this turbulence/chemistry interaction, different possibilities have been attempted in the literature. One of them is to use the Eddy Break-up and Eddy Dissipation Concept. They are based on the phenomenological analysis of turbulent combustion assuming high Reynolds ($Re >> 1$) and large Damköhler ($Da >> 1$) numbers. The first one defines the degree of turbulence and the second one defines a quotient between the flow and the chemical time scales (so, a large Damköhler means "fast chemistry"). Spalding [22] provided an early attempt to the chemical source term closure. Since turbulent mixing may be viewed as a cascade process from the integral down to the molecular scales, the cascade process also controls the chemical reactions as long as mixing rather chemistry is the rate-determining process [1]. A simple idea is to consider that chemistry does not play any explicit role, while turbulent motions control the reaction rate. Then, the mean reaction rate is mainly controlled by a characteristic turbulent time. This model is the Eddy Break-Up (EBU) and it was formulated primarily for premixed combustion. The turbulent mean reaction rate of products q_{Pr} can be expressed as:

$$q_{Pr} = \overline{\rho} C_{EBU} \frac{\widetilde{\epsilon}}{\widetilde{k}} \left(\overline{Y_{Pr}''^{\,2}} \right)^{1/2} \tag{4.29}$$

where C_{EBU} is the Eddy Break-Up constant and $\overline{Y_p''^2}$ is the variance of the product mass fraction. Here $\widetilde{\epsilon}/\widetilde{k}$ is the inverse of a turbulent time scale.

The Eddy Dissipation Concept model, introduced by Magnussen and Mjertager [7], directly extends the Eddy Break-Up model to non-premixed combustion. The fuel mean burning rate is estimated from Favre-averaged fuel, oxidiser and products molar concentrations [X], and depends on a turbulent mixing time estimated also by $\widetilde{\epsilon}/\widetilde{k}$. Then, the following expression is written:

$$q_j^{mix} = C_{EDC} \frac{\widetilde{\epsilon}}{\widetilde{k}} min \left(\frac{\widetilde{[X_{r,j}]}}{\nu_{r,j}}, B \frac{\sum_p^{N_{p,j}} \widetilde{[X_{p,j}]} M_p}{\sum_p^{N_{p,j}} \nu_{p,j} M_p} \right) \tag{4.30}$$

where C_{EDC} and B are modelling constants; $\widetilde{[X_{r,j}]}$, $\widetilde{[X_{p,j}]}$ are Favre-averaged molar concentrations of reactives and products respectively, and $\nu_{r,j}$ and $\nu_{p,j}$ are stoichiometric coefficients of reactives and products respectively of *jth* reaction. Finally, $N_{p,j}$ is the number of products present in *jth* reaction.

These models are usually used for reduced chemistry and are difficult to be extended to full chemistry mechanisms. Nevertheless, different attempts to incorporate reduced mechanisms and full chemistry mechanisms have been published in the literature (see for example [23–25]). Among others, some extended EDC models evaluate the rate determining process comparing the slowest between the mixing process found with Eq. 4.30 and the kinetically controlled process by means of the Arrhenius rate for the same reaction [24, 26]. Then, the expression for a given *jth* reaction can be written as follows:

$$q_j = min\left(q_j^{mix}, q_j^{Arr}\right) \tag{4.31}$$

where, for the *jth* reaction, q_j^{mix} is the mixing controlled reaction rate and q_j^{Arr} is the kinetics controlled reaction rate evaluated by means of Eq. 1.23. The forward and backward rate constants (k_j^f and k_j^b) are evaluated with the modified Arrhenius law and the use of the equilibrium constant K_c, as it is exposed in section 1.3.5. In order to evaluate the reaction rate q_j^{Arr} and the rate constants k_j^f and k_j^b, Favre-averaged temperature and Favre-averaged molar concentrations are considered.

Finally, the net rate of production/destruction of *ith* species is evaluated:

$$\overline{\dot{w}_i} = M_i \sum_{j=1}^{N_R} \left(\nu_{i,j}^{''} - \nu_{i,j}^{'}\right) q_j \tag{4.32}$$

The basic idea is that, in regions with high-turbulence levels, the eddy lifetime $\widetilde{\epsilon}/\widetilde{k}$ is short, so mixing is fast and, as a result, the reaction rate is not limited by small-scale mixing. In this limit, the kinetically controlled reaction rate usually has the smallest value. On the other hand, in regions with low-turbulence levels, small scale mixing may be slow and limits the reaction rate. In this limit, the mixing rates are more important. One weakness of this model is that kinetically controlled reaction rate is calculated using mean quantities of temperatures and mass fractions. In the present thesis, the extended Eddy Dissipation Concept model exposed above is used and is referred as **EDC**.

4.5 The laminar flamelet concept for turbulent non-premixed flames

The main advantage of the flamelet concept is the fact that chemical time and length scales do not need be solved when calculating the flame [27], being calculated in a pre-processing task. The use of this concept and methodology for turbulent combustion allows to calculate temperature and species without solving species and energy transport equations (Eqns. 4.13 and 4.15) and in this way, avoiding an explicit modelization of the time-averaged chemical reaction rates $\overline{\dot{w}_i}$.

For the application of the flamelet concept in turbulent flames, the basic assumption to be considered is that the flame thickness must be smaller than the smallest turbulence length scale, the Kolmogorov length scale, usually denoted by η. Since the chemical time scale is short, chemistry is more active within a thin layer, namely the fuel consumption or inner region. If this layer is thin compared to the size of Kolmogorov eddies, it is embedded within the quasi-laminar flow field of such an eddy and the assumption of a laminar flamelet structure is justified. If, on the contrary, turbulence is so intense that Kolmogorov eddies become smaller than the inner layer and can penetrate into it, they are able to destroy its structure and the entire flame is likely to extinguish [1].

In the previous chapter, and in order to analyse the performance of the laminar flamelet concept, these models have been applied to the multidimensional numerical simulation of laminar non-premixed flames. When solving the flames, a transport equation for the conserved scalar Z is solved together with momentum and continuity equations. Temperature T and species mass fractions Y_i are related to the conserved scalar Z and its instantaneous dissipation rate χ. All scalars are known functions of these two variables and are available in the form of flamelet libraries $\phi(Z, \chi)$.

When solving turbulent flames by means of RANS techniques, the conserved scalar is decomposed in two parts: its mean value and its fluctuation. Being flamelet libraries interpreted as the relationship among instantaneous values of scalar variables respect to the instantaneous values of Z and χ, further modelization is needed to take into account Z and χ fluctuations. Thus, the statistical distribution of Z and χ has to be considered to calculate statistical moments of the scalar variable T and Y_i, such as their mean (or Favre) and their variance. These statistical distributions are the probability density functions (pdf) of the random variables. Information of the Favre-averaged mixture fraction $\widetilde{Z}$ and its variance $\widetilde{Z''^2}$ is required in this point. In addition, information about the Favre-averaged of the scalar dissipation rate $\widetilde{\chi}$ and a further assumption about its fluctuation is also necessary. Once these information is known or assumed, flamelet libraries are integrated and stored.

4.5.1 Favre-averaged conserved scalar equation. Mixture fraction

In addition to the Favre-averaged equations of continuity, momentum, and turbulent quantities such as $\widetilde{k}$ and $\widetilde{\epsilon}$, a Favre-averaged mixture fraction $\widetilde{Z}$ equation and a Favre equation for its variance $\widetilde{Z''^2}$ have to be considered. From Eq. 3.1, the Favre-averaged equation for the mixture fraction can be written as follows [1, 27]:

$$\frac{\partial\left(\overline{\rho}\widetilde{Z}\right)}{\partial t} + \nabla\cdot\left(\overline{\rho}\widetilde{\vec{v}}\widetilde{Z}\right) = \nabla\cdot\left(\overline{\rho D_z \nabla Z}\right) - \nabla\cdot\left(\overline{\rho}\widetilde{v''Z''}\right) \tag{4.33}$$

To obtain a Favre equation for the mixture fraction variance, the following procedure can be applied: subtract the instantaneous equation for the mixture fraction (Eq. 3.1) and its Favre-averaged equation (Eq. 4.33), multiplying the result by $2\widetilde{Z''^2}$ and averaging [1]:

$$\begin{aligned}\frac{\partial\left(\overline{\rho}\widetilde{Z''^2}\right)}{\partial t}+\nabla\cdot\left(\overline{\rho}\widetilde{\vec{v}}\widetilde{Z''^2}\right)=&\nabla\cdot(\overline{\rho D_z\nabla Z''^2})-2\overline{\rho}\widetilde{\vec{v''}Z''}\cdot\nabla\widetilde{Z}\\&-\nabla\cdot(\overline{\rho}\widetilde{\vec{v''}Z''^2})-\overline{2\rho D_z\nabla Z''\cdot\nabla Z''}\end{aligned}\tag{4.34}$$

In equation 4.34, the first term on the r.h.s is due to the molecular spatial diffusion, the second is a production term by the mean gradient, and the third is a diffusion term due to velocity fluctuations. The last term on the r.h.s is the scalar dissipation rate of the fluctuations of the mixture fraction field. This scalar dissipation rate measures the decay of $\widetilde{Z''^2}$.

In order to relate the scalar dissipation rate defined in Chapter 3 for laminar flames with this last term, the Favre-average of expression 3.4 can be written as follows:

$$\begin{aligned}\overline{\rho}\widetilde{\chi}=&\overline{2\rho D_z\nabla\widetilde{Z}\cdot\nabla\widetilde{Z}}+\overline{4\rho D_z\nabla Z''\cdot\nabla\widetilde{Z}}+\overline{2\rho D_z\nabla Z''\cdot\nabla Z''}\approx\\&2\overline{\rho}\overline{D_z}\nabla\widetilde{Z}\cdot\nabla\widetilde{Z}+\overline{2\rho D_z\nabla Z''\cdot\nabla Z''}\end{aligned}\tag{4.35}$$

In [12], these two terms are defined. The first one measures the scalar dissipation rate due to the mean $\widetilde{Z}$ field, while the second one measures the scalar dissipation rate due to the turbulent fluctuations of Z (Z'' field). Neglecting mean gradients against fluctuations gradients, as usually done in RANS [1, 12, 28], the mean of the scalar dissipation rate $\widetilde{\chi}$ can be written as:

$$\overline{\rho}\widetilde{\chi}\approx\overline{2\rho D_z\nabla Z''\cdot\nabla Z''}\tag{4.36}$$

In fact, this scalar dissipation rate of the fluctuations of the mixture fraction field plays for the mixture fraction $\widetilde{Z}$ the same role as the dissipation rate of the kinetic energy $\widetilde{\epsilon}$ for the velocity field. This analogy is often used in the context of RANS models to model this variable with the turbulent mixing time $\widetilde{k}/\widetilde{\epsilon}$:

$$\widetilde{\chi}=c_\chi\frac{\widetilde{\epsilon}}{\widetilde{k}}\widetilde{Z''^2}\tag{4.37}$$

Here c_χ is assumed to be a constant, usually $c_\chi=2.0$. This relation simply expresses that scalar dissipation time and turbulence dissipation time are proportional [12].

$$\frac{\widetilde{Z''^2}}{\widetilde{\chi}}=\frac{1}{c_\chi}\frac{\widetilde{k}}{\widetilde{\epsilon}}\tag{4.38}$$

Other possibilities are described in the literature. A common strategy is to derive a modelled transport equation for the Favre-averaged scalar dissipation $\widetilde{\chi}$ rate itself. This analysis is beyond the scope of the present thesis. See [1] for further information.

The scalar turbulent fluxes for the transport equations 4.33 and 4.34 are modelled by the *simple gradient diffusion hypothesis* and can be written as:

$$\overline{\rho}\widetilde{\vec{v}''Z''} = -\frac{\mu_t}{\sigma_Z}\nabla\widetilde{Z} \tag{4.39}$$

$$\overline{\rho}\widetilde{\vec{v}''Z''^2} = -\frac{\mu_t}{\sigma_{Z''^2}}\nabla\widetilde{Z''^2} \tag{4.40}$$

where the turbulent Prandtl numbers σ_Z and $\sigma_{Z''^2}$ are constants of the model.

The time-averaged molecular fluxes (first term at the r.h.s of Eq. 4.33 and first term at the r.h.s of Eq. 4.34) are modelled with the procedure described in section 4.4.4, where the instantaneous variables are simply substituted by their Favre-averaged value.

4.5.2 Mean scalars and scalar variances

In the context of flamelet modelling, scalars such as species mass fractions and temperature depend only on the mixture fraction and the scalar dissipation rate $\phi = \phi(Z, \chi)$ by means of the flamelet equations. In principle, both variables Z and χ are instantaneous quantities and their statistical distribution needs to be considered in order to calculate statistical moments of the reactive scalars. Therefore, knowing the joint Favre probability density function $\widetilde{P}(Z, \chi)$ of Z and χ and taking into account Eq. 4.1 and 4.2, the mean $\widetilde{\phi}$ and the variance $\widetilde{\phi''^2}$ of a generic scalar ϕ might by evaluated by:

$$\widetilde{\phi} = \int_0^1 \int_0^\infty \phi(Z, \chi)\widetilde{P}(Z, \chi)d\chi dZ \tag{4.41}$$

$$\widetilde{\phi''^2} = \int_0^1 \int_0^\infty (\phi(Z, \chi) - \widetilde{\phi})^2\widetilde{P}(Z, \chi)d\chi dZ \tag{4.42}$$

The joint Favre pdf can be calculated deriving a transport equation or alternatively, taking into account a presumed distribution. In this thesis, the second alternative is considered.

First of all, statistical independence of Z and χ is assumed ($\widetilde{P}(Z, \chi) \approx \widetilde{P}(Z)\widetilde{P}(\chi)$). Different alternatives are explored in the literature for both the pdf, i.e. of the scalar dissipation rate $\widetilde{P}(\chi)$ and the mixture fraction $\widetilde{P}(Z)$. For the scalar dissipation rate, a log-normal function can be assumed [29]. However, the most common assumption is to ignore the fluctuations of the scalar dissipation rate and to use flamelet profiles

with scalar dissipation rates corresponding to the mean value $\widetilde{\chi}$ found locally in the turbulent flow [27]. This approximation is used in the present thesis. Then, the only Favre pdf required to be presumed is for the mixture fraction. This pdf is considered to be controlled by its first two moments, say the Favre-averaged mixture fraction and the Favre-averaged variance of the mixture fraction. For non-premixed turbulent flames, the probability density function commonly used is the beta function [1]:

$$\widetilde{P}(Z) = \frac{Z^{\alpha-1}(1-Z)^{\beta-1}}{\Gamma(\alpha)\Gamma(\beta)}\Gamma(\alpha+\beta) \tag{4.43}$$

Here Γ is the gamma function. The two parameters α and β are related to the Favre mean $\widetilde{Z}$ and the variance $\widetilde{Z''^2}$ by $\alpha = \widetilde{Z}\gamma$ and $\beta = (1-\widetilde{Z})\gamma$, where $\gamma = \frac{\widetilde{Z}(1-\widetilde{Z})}{\widetilde{Z''^2}} - 1 \geq 0$.

Therefore, Favre-averaged temperature and species mass fractions are evaluated solving the following integrals:

$$\widetilde{T}(\widetilde{Z}, \widetilde{Z''^2}, \widetilde{\chi}) \approx \int_0^1 T(Z, \widetilde{\chi})\widetilde{P}(Z)dZ \tag{4.44}$$

$$\widetilde{Y_i}(\widetilde{Z}, \widetilde{Z''^2}, \widetilde{\chi}) \approx \int_0^1 Y_i(Z, \widetilde{\chi})\widetilde{P}(Z)dZ \tag{4.45}$$

The Favre-averaged scalar dissipation rate $\widetilde{\chi}$ is also needed in equations 4.44 and 4.45. Integrating the scalar dissipation rate with the probability density function of Z, the following expression can be written:

$$\widetilde{\chi} = \int_0^1 \chi(Z)\widetilde{P}(Z)dZ \tag{4.46}$$

Here, $\chi(Z)$ is introduced depending on the modelization employed for the scalar dissipation rate dependence on the mixture fraction. In the previous chapter, different criteria have been analysed and compared: $\boldsymbol{\chi_1}$, $\boldsymbol{\chi_2}$ and $\boldsymbol{\chi_3}$.

In addition, and considering that the mass-weighted pdf is related to the unweighted pdf through the expression:

$$\widetilde{P}(Z) = \frac{\rho}{\widetilde{\rho}}P(Z) \tag{4.47}$$

the mean density $\overline{\rho}$ can be taken from [1, 27]:

$$\frac{1}{\overline{\rho}} = \int_0^1 \rho^{-1}(Z, \widetilde{\chi})\widetilde{P}(Z)dZ \tag{4.48}$$

Models for the scalar dissipation rate dependence on the mixture fraction

As exposed, the scalar dissipation rate dependence on mixture fraction has to be modelled. In the previous chapter of the present thesis, the **analytical approximation** for the counter-flow diffusion flame or the one-dimensional laminar mixing layer reported in [1, 29] has been referred as **Criterion $\boldsymbol{\chi_1}$**:

$$\chi = \chi_{st}\frac{\Phi}{\Phi_{st}}\frac{f(Z)}{f(Z_{st})} \qquad \text{with} \qquad \Phi = \frac{1}{4}\frac{3\left(\sqrt{\rho_\infty/\rho}+1\right)^2}{2\sqrt{\rho_\infty/\rho}+1} \tag{4.49}$$

where Z_{st} is the stoichiometric mixture fraction; Φ is a factor introduced in order to consider variable density effects [30]; the subscript ∞ means the oxidiser stream and $f(Z)$=exp $\left[-2\left[erfc^{-1}\left(2Z\right)\right]^2\right]$ with $erfc^{-1}$ is the inverse of the complementary error function. Using this expression in the flamelet equations, the flamelet library is built with two input parameters: Z and χ_{st}. See section 3.2.3 for further information.

Using this criterion $\boldsymbol{\chi_1}$, the equation 4.46 for the Favre-averaged scalar dissipation rate $\widetilde{\chi}$ can be written as follows:

$$\widetilde{\chi} = \frac{\widetilde{\chi_{st}}}{\Phi_{st}f(Z_{st})}\int_0^1 \Phi f(Z)\widetilde{P}(Z)dZ \tag{4.50}$$

Then, using expression 4.37 and 4.50 the Favre-averaged scalar dissipation rate at stoichiometric conditions $\widetilde{\chi}_{st}$ can be expressed as follows:

$$\widetilde{\chi}_{st} = \frac{c_\chi \frac{\widetilde{\epsilon}}{\widetilde{k}}\widetilde{Z''^2}}{\frac{1}{\Phi_{st}f(Z_{st})}\int_0^1 \Phi f(Z)\widetilde{P}(Z)dZ} \tag{4.51}$$

Otherwise, when a **constant** scalar dissipation rate at stoichiometric conditions (**criterion $\boldsymbol{\chi_2}$**) is used, the Favre-averaged scalar dissipation rate at stoichiometric conditions reduces to:

$$\widetilde{\chi}_{st} = c_\chi \frac{\widetilde{\epsilon}}{\widetilde{k}}\widetilde{Z''^2} \tag{4.52}$$

Therefore, both $\boldsymbol{\chi_1}$ and $\boldsymbol{\chi_2}$ use $\widetilde{\chi}_{st}$ as an external parameter to evaluate the Favre-averaged temperature and species mass fractions :

$$\widetilde{T}(\widetilde{Z}, \widetilde{Z''^2}, \widetilde{\chi_{st}}) \approx \int_0^1 T(Z, \widetilde{\chi_{st}})\widetilde{P}(Z)dZ \tag{4.53}$$

$$\widetilde{Y_i}(\widetilde{Z}, \widetilde{Z''^2}, \widetilde{\chi_{st}}) \approx \int_0^1 Y_i(Z, \widetilde{\chi_{st}})\widetilde{P}(Z)dZ \tag{4.54}$$

On the other hand, the **interactive strategy** referred in the previous chapter as **Criterion χ_3** requires the $\widetilde{\chi}$ profile evaluated in the actual flame simulation. With Eq. 4.37 the profiles are evaluated, and this in situ information is used to recalculate the flamelet library.

4.6 Research approach

The aim of the research hereafter presented is to numerically investigate the adequacy of the application of the laminar flamelet concept on the numerical simulation of multidimensional turbulent non-premixed flames. Numerical solutions are compared to experimental data available in the literature paying special attention to the prediction of pollutant formation.

Steady and unsteady flamelet simulations are studied and compared taking advantage of the knowledge and experience achieved in the previous chapter of the present thesis. Steady flamelet are used considering unity-Lewis numbers for each species and adiabatic flame conditions (no radiation). On the other hand, unsteady flamelets are employed in order to simulate differential diffusion effects as well as radiation heat transfer. Also, an extended Eddy Dissipation Concept model (here referred with the acronym EDC) using an irreversible single-step reaction, and with a reduced mechanism (four-step) is compared to the previously cited flamelet modelling simulations. Regarding the turbulent model, the standard high Reynolds $\widetilde{k}-\widetilde{\epsilon}$ turbulence model is used given the nature of the test selected (open boundaries, i.e. no wall effects). The round-jet anomaly is taken into account and the influence of different values of the model constant $c_{\epsilon 2}$ exposed in the literature are investigated in section 4.8.3.

Verified numerical solutions are presented in order to validate the performance and adequacy of the mathematical models exposed above. The verification procedure used establishes criteria on the sensitivity of the simulation to the computational model parameters that account for the discretization, i.e. the mesh spacing and the numerical schemes. This tool estimates the order of accuracy of the numerical solution (observed order of accuracy p), and the error band where the grid independent solution is expected to be contained (uncertainty due to discretization GCI), also giving criteria on the credibility of these estimations [31–33]. Furthermore, the validation process (adequacy of the mathematical formulation employed) is performed with available experimental data of the test case selected since the computational cost of detailed simulations based on the full resolution of the transport governing equations (DNS simulation with the full integration of the energy and species equations) is prohibitive for the majority of cases.

4.6.1 Test case

The so-called Flame D [9], a turbulent piloted methane/air jet flame, has been selected as the test case given the extensively experimental data available in the literature and the simple geometry and flow configuration. This flame is under the framework of the *International Workshop on Measurement and Computation of Turbulent Non-premixed Flames* (TNF) [8], and belongs to a series of flames (from A to F) with the same geometry configuration but different Reynolds numbers. Flame D has a fuel stream based Reynolds number of Re=22400. At these flow conditions, the flame burns as a diffusion flame and no evidence of premixed reaction in the fuel-rich methane/air mixture was found. Moreover, it has a small degree of local extinction. Experimental data is extensively reported in [8].

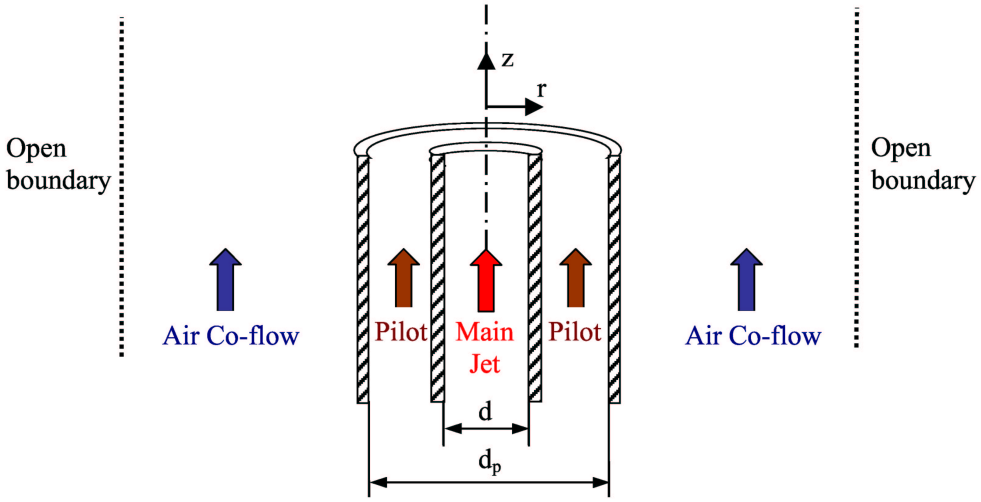

Figure 4.1: Piloted non-premixed methane/air turbulent flame. Burner scheme.

The piloted burner has a main jet inner diameter of d=7.2 mm and a piloted annulus inner diameter of 7.7 mm (wall thickness w_i=0.25 mm). Piloted annulus outer diameter is d_p=18.2 mm with a burner outer wall diameter of 18.9 mm (wall thickness w_o=0.35 mm). The main jet composition is, in volume, a 25% of CH_4 and 75% of dry air, with a temperature of 294 K and a mean velocity of 49.6 m/s ($\pm$ 2 m/s), which, as mentioned above, leads to a fuel stream based Reynolds number of Re=22400. Fig. 4.1 shows a scheme of the burner configuration.

In the experiments performed by Barlow and Frank [9], the pilot composition and temperature was adjusted such that the pilot stream has the same equilibrium

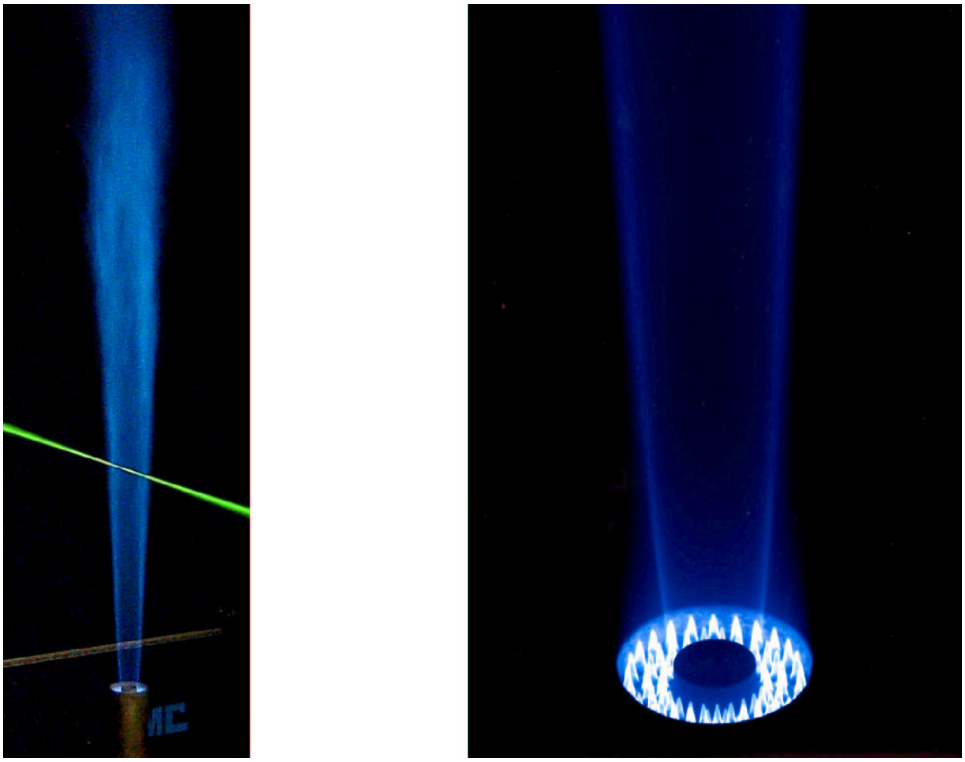

Figure 4.2: Piloted non-premixed methane/air turbulent flame: Left: Flame D with a laser beam; Right: Close-up of Flame D. These images are used with permission of the authors [8].

composition as a mixture fraction of $Z = 0.27$, which is slightly lean ($\phi = 0.77$) compared with a stoichiometric mixture fraction of $Z_{st} = 0.351$. Then, the annular pilot burns a lean mixture of C_2H_2, H_2, air, CO_2 and N_2 with the same nominal enthalpy and equilibrium composition as methane/air at $Z = 0.27$.

The flame stabiliser in the pilot is recessed below the burner exit, such that burnt gas is at the exit plane as shown in Fig. 4.2. The compositional boundary condition in the pilot, described in [8] for flame D, was determined by matching the measurements at z/d=1 with calculations (by J-Y Chen) of laminar unstrained premixed CH4/air flames and then extrapolating to the conditions at burner exit plane, based on the estimated convective time up to z/d=1. The pilot burnt gas velocity is determined from the cold mass flow rate, the density at the estimated exit condition, and the flow area of the pilot annulus. Separate calculations were performed to demonstrate that there are negligible differences in burnt gas composition for the pilot mixture vs. CH_4/air at the same total enthalpy and equivalence ratio [8].

The pilot composition measured in the (nearly) flat portion of the radial profile at z/d=1 in flame D is [8]: $\phi = 0.77$, $Z = 0.27$, $Y_{N_2} = 0.734$, $Y_{O_2} = 0.056$, $Y_{H_2O} = 0.092$, $Y_{CO_2} = 0.110$, $Y_{OH} = 0.0022$.

4.6.2 Mathematical models

Flamelet modelling approaches for turbulent combustion with a presumed PDF

The Favre-averaged equations of continuity (Eq. 4.12), momentum (Eq. 4.14), mixture fraction and its variance (Eqns. 4.33 and 4.34), turbulent kinetic energy and the dissipation of the turbulent kinetic energy (Eqns. 4.21 and 4.22) are considered. The Favre-averaged of the scalar dissipation rate is evaluated by means of Eq. 4.46. Favre-averaged mass fraction of species, temperature and density are obtained from the integrated flamelet libraries.

Steady flamelets (**SF**) and unsteady flamelets (**UF**) have been used and compared. The detailed chemical mechanism GRI-Mech 3.0 [34] is considered for all the flamelet modelling simulations. Laminar flamelet libraries are evaluated with the **Complete formulation** defined in the previous chapter (Eqn. 3.2 and 3.3) since, in general, they provide better results than simplified alternatives. Regarding the scalar dissipation rate modelling, two possibilities described in section 3.2.3 are used: the analytical approximation ($\boldsymbol{\chi_1}$) for steady flamelets, and the interactive strategy ($\boldsymbol{\chi_3}$) for unsteady flamelets. Finally, the characteristic velocity used to calculate the flamelet lifetime required for the unsteady flamelet simulations is evaluated by the averaged velocity ($\boldsymbol{\tau_2}$) following the strategy proposed in section 3.2.4. The flamelet libraries have been integrated by means of Eqns. 4.44, 4.45 and 4.48 and assuming a beta function pdf.

Eddy Dissipation Concept (EDC) models

The Favre-averaged equations of continuity, species, momentum, and energy (Eqns. 4.12-4.15) as well as a transport equations for the turbulent kinetic energy and the dissipation of the turbulent kinetic energy (Eqns. 4.21 and 4.22) are considered. Eq. 4.32 is used to close the problem.

Two chemical mechanism are taken into account with the extended Eddy Dissipation Concept model described in section 4.4.6: an irreversible single-step mechanism [35], referred as **SS**, which involves five species (CH_4, $O2$, CO_2, H_2O and N_2) and a four-step mechanism of Jones & Lindstedt [36] which involves seven species (CH_4, $O2$, CO_2, H_2O, H_2, CO and N_2) referred as **4S**. The EDC empirical constants for the evaluation of the time-averaged reaction rate $\overline{\dot{w}_i}$ with Eq. 4.32 are set to C_{EDC}=4 and B=0.5. These values are recommended for the original reference by Magnussen and Mjertager [7].

Turbulence model

Given the nature of the flame studied (open boundaries, then no solid walls create low-Reynolds number effects), the standard $\widetilde{k}-\widetilde{\epsilon}$ model is applied [17] considering a slight modification to take into account the round-jet anomaly. A high Reynolds version of this eddy-viscosity model is assumed to be enough since it is an unconfined flame with no walls in all the domain. The following functions and constants are taken into account: $f_\mu = f_1 = f_2 = 1$, $C_\mu = 0.09$, $c_{\epsilon 1} = 1.44$, $c_{\epsilon 2} = 1.80$, $\sigma_k = 1.0$ and $\sigma_\epsilon = 1.3$. The turbulent Prandtl numbers for energy and species used in Eqn. 4.18 and 4.19 are $\sigma_h = \sigma_{Y_i} = 0.9$. The turbulent Prandtl numbers for the mixture averaged and its variance are considered σ_Z=$\sigma_{Z''^2}$=0.7. The coefficient on the modelling of the mean of the scalar dissipation rate is set to c_χ=2.0.

Given the configuration of the turbulent flame studied, and in order to take into account the round-jet anomaly described in the literature [19], the modification of the $c_{\epsilon 2}$ described in some posters presented in [8] is used. The standard value is $c_{\epsilon 2}$=1.92 and is modified by $c_{\epsilon 2}$=1.8. A comparison of the performance of both values is shown in section 4.8.3.

Thermo-physical properties and radiation sub-model

Thermo-physical properties and transport coefficients are evaluated with the same procedure described in section 3.3.2. Mixture diffusion coefficients $\mathcal{D}_{im}$ are calculated considering the possibilities of a fixed Lewis number (Le_i=*constant*) for each species or the assumption of unity-Lewis number for all the species involved in the chemical model (Le_i=1.0, $i = 1, 2, ...N$). An optically thin radiation model [32, 37, 38] is adopted in the same way as exposed in section 3.3.2.

Boundary conditions

The main jet composition is, in volume, a 25% of CH_4 and 75% of dry "regular" air, with a temperature of 294 K and a mean axial velocity of 49.6 m/s. See Fig. 4.3 for the inlet axial velocity profile. The radial velocity is null. A unity mixture fraction is considered and a null variance of the mixture fraction is assumed.

The piloted jet velocity is 11.4 m/s (experimental measure uncertainties ± 0.5 m/s). The pilot composition at the burner exit is taken as that of an unstrained CH4/air premixed flame at the point in the flame profile where T=1880 K (experimental measure uncertainties ± 50 K), following the process outlined above. The boundary conditions of the pilot are: ϕ = 0.77, Z = 0.27, T = 1880 K, ρ = 0.180 kg/m^3, Y_{N_2}=0.7342, Y_{O_2}=0.0540, Y_O=7.47e-4, Y_{H_2}=1.29e-4, Y_H=2.48e-5, Y_{H_2O}=0.0942, Y_{CO}=4.07e-3, Y_{CO_2}=0.1098, Y_{OH}=0.0028, Y_{NO}=4.8e-6. The mixture fraction variance is considered null.

Finally, there is a co-flow of "regular" air with a velocity of 0.9 m/s (experimental measure uncertainties ± 0.05 m/s) and a temperature of 291 K. See more details in [8]. The mixture fraction and its variance are considered null.

Boundary conditions for the turbulent kinetic energy $\widetilde{k}$ and for the dissipation of the turbulent kinetic energy $\widetilde{\epsilon}$ as well as the profile of the inlet axial velocity are provided by [8] (see Fig. 4.3).

At the upper outlet of the computational domain, a pressure outflow boundary condition is imposed [39], and a null gradient in the axial direction of all the scalars (temperature, species, turbulent kinetic energy and its dissipation and mixture fraction and its variance) is assumed. Otherwise, at the maximum radius considered in the computational domain, a null radial velocity is assumed and a null gradient of the axial velocity and all the scalar quantities is considered.

4.7 Numerical methodology

The mathematical model is discretized using the finite volume technique on cylindrical staggered grids. Central differences are employed for the evaluation of the diffusion terms, while a first order upwind scheme is used for the evaluation of the convective ones [40]. A time-marching SIMPLE-like algorithm is employed to couple velocity-pressure fields [40]. Discretized equations are solved in a segregated manner using a multigrid solver [41]. The convergence of the time-marching iterative procedure is truncated once normalised residuals are below 10^{-8}.

The computational domain extends from z/d=0 to z/d=100 and from r/d=0 to r/d=20. Here, z is the axial coordinate and r is the radial coordinate.

Domain decomposition method is used as a strategy to reduce the number of grid nodes far from the flame fronts, and as a parallelisation technique. For further details